

## Preparation, Characterization, and Antimicrobial Activity of Polyaniline and Fe<sub>2</sub>O<sub>3</sub>/Polyaniline Composite Nanoparticle

Nather Ibraheem Mohamed<sup>a1\*</sup>, Salma M. Hassan<sup>b1</sup>, Khaleed J. Khalil<sup>c2</sup>

<sup>1</sup>Department of Physics, College of Science, University of Baghdad, Baghdad, Iraq

<sup>2</sup>Iraqi Center for Cancer and Medical Genetics Research, Mustansiriyah University, Baghdad, Iraq

<sup>b</sup>E-mail: Salma.mhammed@yahoo.com, <sup>c</sup>E-mail: khaleedkhalil59@gmail.com

<sup>a\*</sup>Corresponding author: natheri1990@gmail.com

### Abstract

An oxidative polymerization approach was used to create polyaniline (PANI) and Fe<sub>2</sub>O<sub>3</sub> /PANI nanoparticle combination. Various characterization approaches were used to investigate the structural, morphological, and Fe<sub>2</sub>O<sub>3</sub> /PANI nanoparticle structures. The findings support the synthesis of polycrystalline nanoparticle PANI and Fe<sub>2</sub>O<sub>3</sub> /PANI spherical nanoparticle composites. Gram-positive bacteria are tested for antibacterial activity. Various quantities of Nanoparticles of PANI and Fe<sub>2</sub>O<sub>3</sub> /PANI nanoparticle composites were used to test Staph-aureus and gram-negative bacteria, E-coli, and candida species. PANI has antibacterial properties against all microorganisms tested. Fe<sub>2</sub>O<sub>3</sub> /PANI nanoparticle composites, on the other hand, have higher antibacterial activity, as evidenced by the zone of inhibition. Bacterial inhibition zones are in S. aureus (positive), and E. coli are in good functioning order. With increasing concentrations of Fe<sub>2</sub>O<sub>3</sub> /PANI nanoparticle composites, the inhibition zones of all bacteria are larger. Finally, the antimicrobial activity of Fe<sub>2</sub>O<sub>3</sub> /PANI nanoparticle composite is characterized using a simplified mechanism based on electrostatic attraction. In this paper, a conductive polymer doped with iron nanoparticles was fabricated for the aim of testing it in the field of bacterial resistance.

### Article Info.

#### Keywords:

Conductive polymer, Fe<sub>2</sub>O<sub>3</sub>/PANI, nanoparticle composite, Antibacterial activities, L-cystien.

#### Article history:

Received: Nov. 09, 2021

Accepted: Jan. 16, 2022

Published: Mar. 01, 2022

## 1. Introduction

PANI Polymer synthesis and characterization have been one of the most important study subjects in polymer and materials science during the last two decades [1]. Because of their environmental resistance [2], tunable electrical conductivity, and intriguing redox properties connected to chain nitrogen, the century-old aniline polymers have attracted attention among electroactive polymers. The general formula for aniline polymers is  $[(-B-NH-B-NH)_y(B-N=Q=N)_{1-y}]_n$ , where B represents a benzenoid ring and Q represents a quinonoid ring. The polymer's intrinsic oxidation state can be varied from wholly reduced leucoemeraldine (LM,  $y = 1$ ) to 50 percent intrinsically oxidized emeraldine (EM,  $y = 0.5$ ) to fully oxidized per nigraniline (PNA,  $y = 0$ ). Crystallinity is also seen in aniline polymers [3].



Polymers have seen significant growth in their utilization in biological applications during the last few decades. Electrical stimulation of cellular processes such as cell proliferation [4] and cell migration has also been proven to tune cellular functions with conductive polymers (CPs). Conducting polymers and their derivatives for tissue engineering applications have sparked a lot of interest. Metals and inorganic semiconductors exhibit electrical and optical properties that are similar to CPs. They do, however, share many of the same appealing qualities as ordinary polymers, such as the convenience of use. In comparison to metals, it has a good synthesis and processing ability. Moreover, Polyaniline (PANI) is one of the most promising biologically active compounds. Due to their one-of-a-kind and distinguishing traits. Numerous investigations on this polymer have been conducted. PANI is one of the most well-characterized conducting polymers; it exhibits a wide variety of structural shapes, excellent environmental stability, and a high capacity for charge transport [5].

Infectious disorders caused by pathogenic bacteria have become a severe public health concern, accounting for about a third of all fatalities worldwide. Antibiotics are the most antibiotics that are frequently given treatment for bacterial infections. On the other hand, antibiotic overuse has resulted in the emergence of multidrug-resistant bacteria such as vancomycin-resistant enterococcus (VRE), vancomycin-resistant *Staphylococcus aureus* (VRSA), and methicillin-resistant *Staphylococcus aureus* (MRSA), all of which pose a significant threat to human health [6]. As a result, alternative bactericidal treatment techniques that are less likely to acquire resistance in microorganisms are urgently needed. Heat at temperatures above 50°C can kill bacteria by denaturing proteins and enzymes or damaging cell membranes. As a result, PANI with oxide ferric has been hailed as one of the most promising new bactericidal therapeutic techniques for fighting *E. coli*, *S. aureus*, and candida bacteria due to its low potential for resistance and toxicity. As a result, this section highlights new study findings on PANI-based materials for bacterial infection eradication [7].

## 2. Experimental work

### 2.1. Polyaniline-Fe<sub>2</sub>O<sub>3</sub> synthesis and modification

From aniline monomer and ammonium persulfate, hydrophobic PANI was produced by oxidative chemical polymerization (APS) as an oxidant, followed by doping with an Fe<sub>2</sub>O<sub>3</sub> in situ polymerization. The hydrophobic emeraldine base polymer was coated with L-cysteine utilizing the nano emulsion process to achieve the required water solubility. In biological media, PANI NPs displayed colloidal stability and NIR absorption that was pH and oxidative environment-dependent. The added ratios are obtained by in-situ polymerization of aniline onto Fe<sub>2</sub>O<sub>3</sub> (Iron (III) oxide and aniline solution with continuous stirring for half an hour with a magnetic stirrer, the added ratios are obtained by in-situ polymerization of aniline onto Fe<sub>2</sub>O<sub>3</sub> (Iron (III) oxide and aniline solution with continuous stirring for half an hour with a magnetic stirrer (0.02 and 0.05 g). were dissolved in a 1M aniline aqueous solution. Ammonium persulfate (APS) (2.5 M) was used as an oxidant to start the polymerization. They were allowed to react for 30 minutes to 2 hours in a 5 °C ice bath. Using a nucleophilic addition procedure, they were functionalized. At room temperature, the powder was submerged in a stirred aqueous solution of 1 M L-cysteine for 24 hours. They were then rinsed with deionized water (DI).

## 2.2. Characterization of chemical structure

The near-IR spectrum ( $400\text{ cm}^{-1}$ ), the mid-IR spectrum ( $400\text{-}4000\text{ cm}^{-1}$ ), and the near-IR spectrum ( $400\text{-}4000\text{ cm}^{-1}$ ) are the IR spectrum's three wavenumber divisions ( $4000\text{-}13000\text{ cm}^{-1}$ ). While the mid-IR scope is the most frequently used for sample analysis, the far- and near-IR bands also provide information about the samples. The purpose of this research was to examine FTIR in the mid-IR spectrum.

To transform infrared spectrophotometer, Fourier calculated the chemical structures of all samples (FTIR). The spectra of the polymer were acquired in transmission mode in air and modified polymer-supported onto PE a Nicolet Impact 410 spectrometer. A total of 200 scans with a resolution of  $4\text{ cm}^{-1}$  were averaged. A Shimadzu UV-2401PC spectrometer was used to record UV-visible spectra in the wavelength range of (250 – 1000) nm.

## 3. Result and discussion

The FTIR spectra of PANI- $\text{Fe}_2\text{O}_3$ -Cys at two different concentrations (0.02 and 0.05) g are shown in Fig.1.  $\text{Fe}_2\text{O}_3$ PANI-Cys (0.02g) (black line) and  $\text{Fe}_2\text{O}_3$ PANI-Cys (0.05g) (red line) FTIR spectra are shown in Fig.1. When comparing the FTIR spectra for L-Cysteine in Figs. 1 and 2, it can be noticed that the intensity has decreased. All of the polyaniline absorption bands were visible in the PANI spectrum:  $1577\text{-}1579\text{ cm}^{-1}$  and  $1502$  (given to C=C-C Aromatic ring stretching) and  $1452\text{-}1413\text{ cm}^{-1}$  (C-H Methyl asym) [8]. The band at  $1305\text{ cm}^{-1}$  corresponding to the stretching vibration of C N, and the band at  $1147\text{ cm}^{-1}$  corresponding to the ring stretching N-Q-N, where Q represents the quinoid ring [9], can also be. The electronic transition in the polymer's free carriers was assigned to a broad conduction band ranging from  $1045\text{ cm}^{-1}$  to  $821\text{ cm}^{-1}$  [10, 11]. Additional absorption bands at  $596\text{-}690\text{ cm}^{-1}$  in the FTIR spectra of modified PANI- $\text{Fe}_2\text{O}_3$  -Cys might be linked to the Alcohol O-H of plane bent. In addition, additional bands at  $972\text{ cm}^{-1}$  and  $825\text{ cm}^{-1}$  correspond to the stretching of cysteine's C-O and C-O groups [12]. PANI-Cys showed new functional properties in the infrared band.

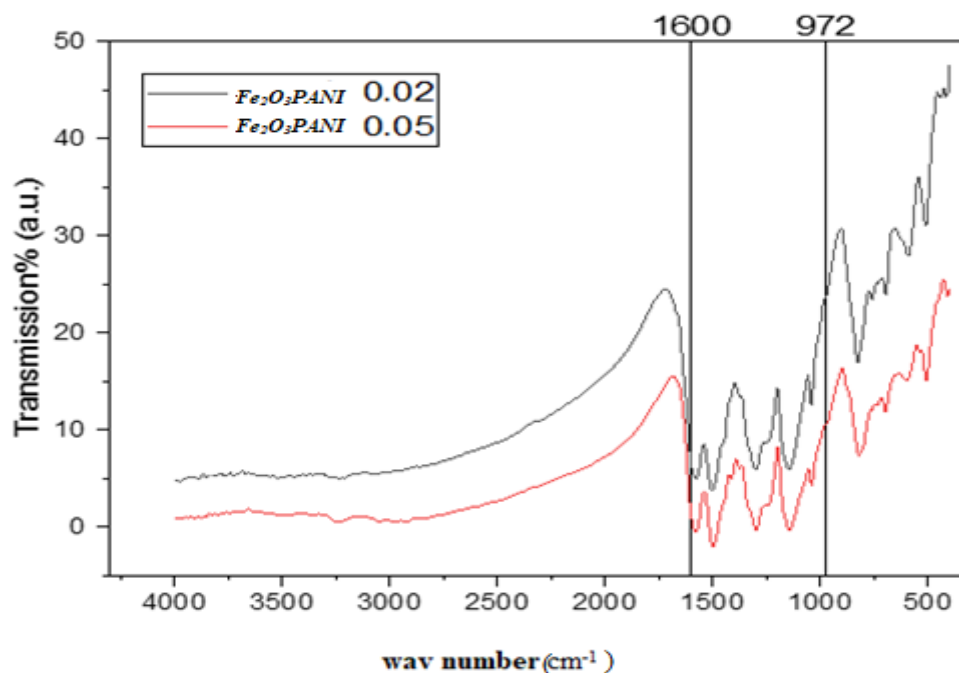
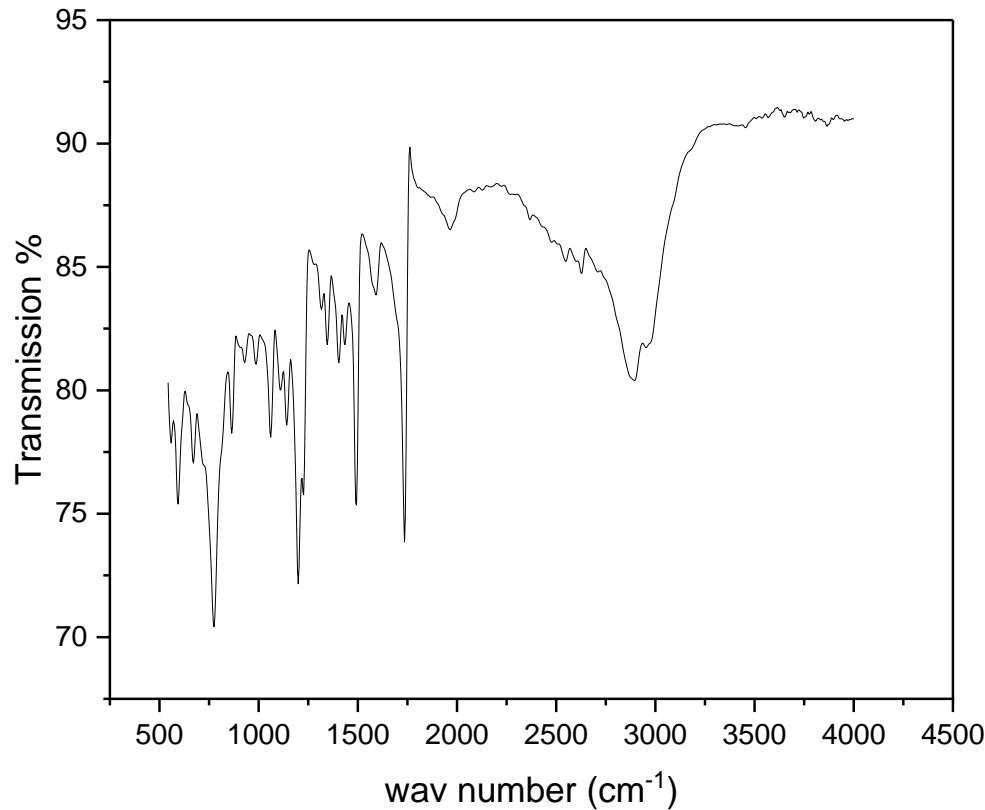


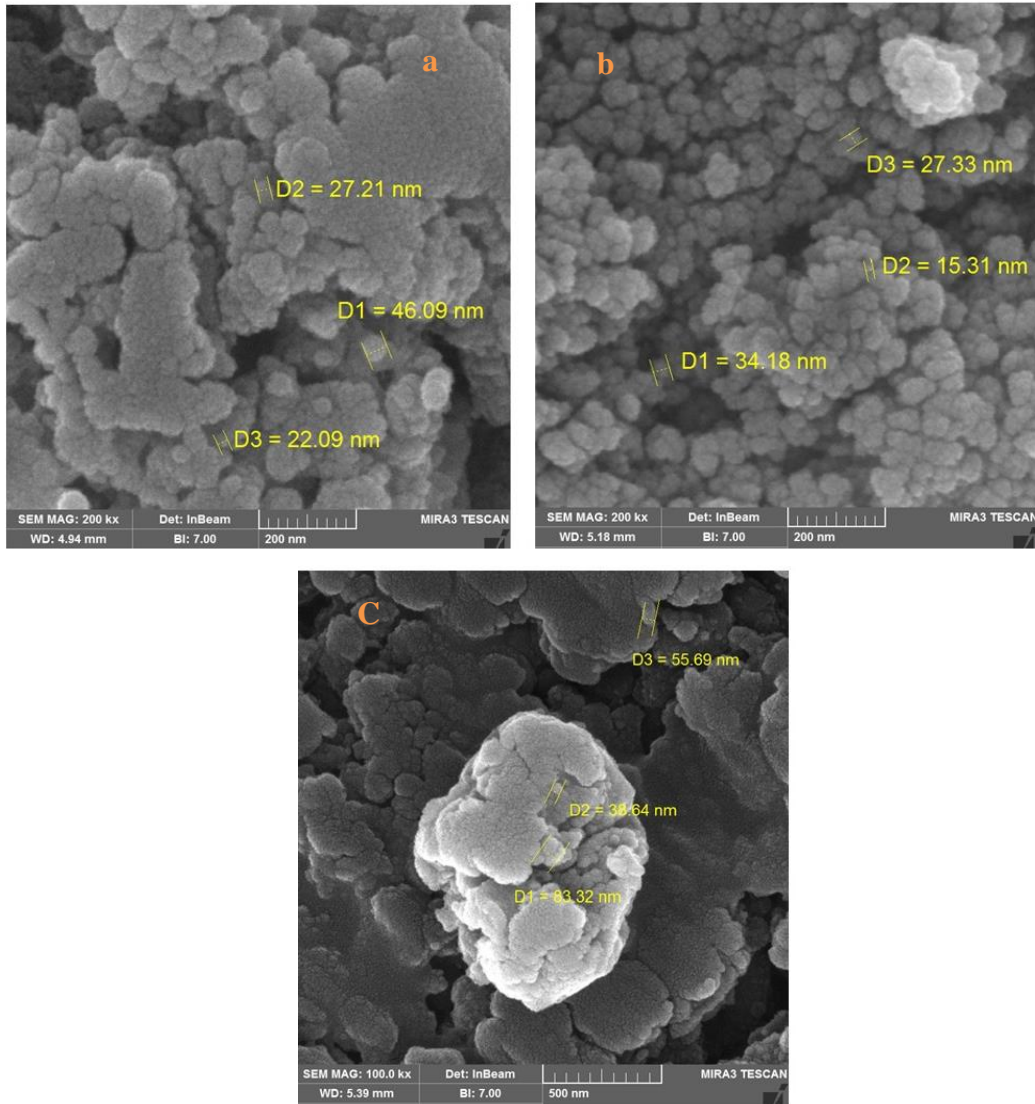
Figure 1: The  $\text{Fe}_2\text{O}_3$ PANI-Cys FTIR spectral areas.



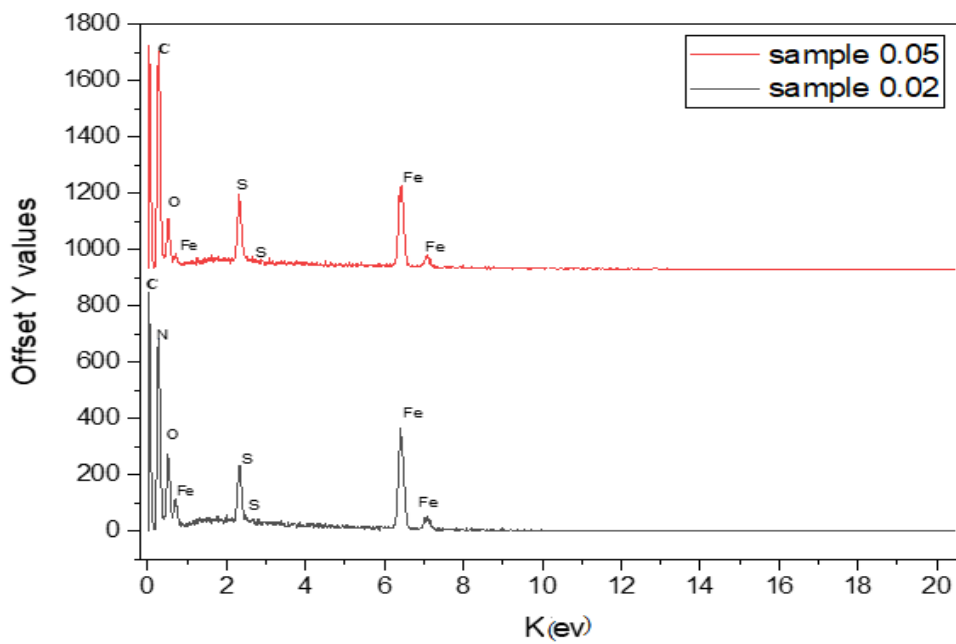
**Figure 2: The FTIR spectrums for PANI-  $Fe_2O_3$  -Cys with L-Cysteine.**

Fig.3(a) shows the FE-SEM morphology of pure PANI. Fig.3(b, c) shows the FE-SEM images picture of ferric Polyaniline (PANI- $Fe_2O_3$ -Cys) powder at concentrations of 0.02 gm and 0.05 gm which demonstrates that the composite is highly microporous and can increase the liquid-solid interfacial area. An FE-SEM analysis [13] corroborated the material's highly porous structure and clumped spherical form. Because of the polymer, the hybrid biomaterial had an uneven surface with particle sizes ranging from 22.9 nm to 46.09 nm for 0.02 gm and 0.05 gm percent.  $Fe_2O_3$  microspheres with a mean diameter of 26 nm worked as a scaffold, enabling numerous micro- or nanopores to be formed where the polymer nanoparticles can fill according to an analysis of SEM images [10, 11].

Many peaks corresponding to carbon (C), sulfur (S), and oxygen (O) are seen in the elemental analysis of PANI-Cys powder, as illustrated in Fig.4, from feature materials of the composite powder of PANI and L-Cystine the ratio of weight % and the atomic percentage was calculated and listed in table 1. Three linear patterns were identified in the components of iron (III) oxide. Thus, it can be observed that the carbon ratio (44.19 percent) has a high proportion (due to its presence in all components) our result agrees with [14, 15].



**Figure 3: FE-SEM morphology of pure PANI. And PANI-Fe<sub>2</sub>O<sub>3</sub>-System.**



**Figure 4: EDX analysis for Polyaniline with iron II dioxide-Cyst powder.**

**Table 1: The proportions for chemical elements.**

Elt	Line	Int	Error	K	Kr	W%	A%	ZAF
C	Ka	178.4	15.75	0.439	0.189	44.19	58.39	0.42
N	Ka	13.8	15.75	0.046	0.019	13.53	15.33	0.14
O	Ka	77.2	15.75	0.094	0.040	19.54	19.38	0.20
S	Ka	73.7	1.10	0.0425	0.018	2.14	1.06	0.85
Fe	Ka	177.4	0.98	0.377	0.163	20.6	5.85	0.79

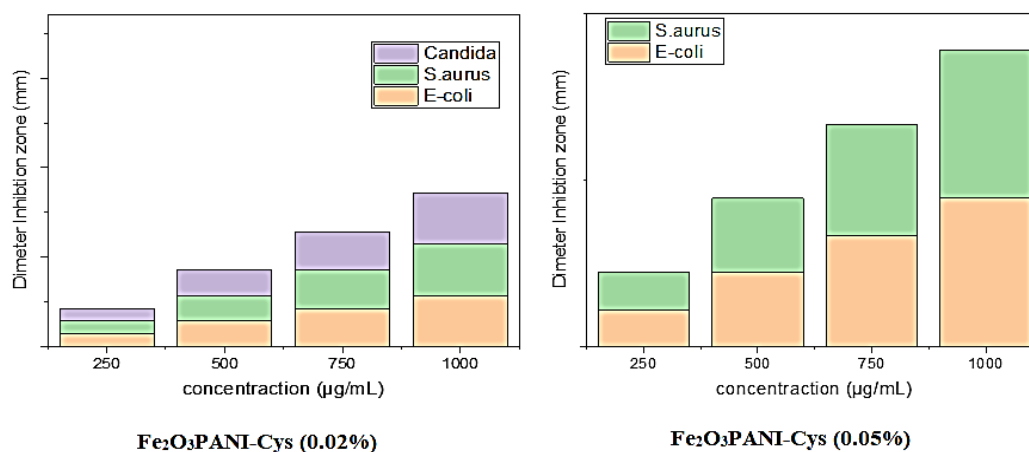
S. aureus, E. coli, and candida were employed in the current investigation. Fig.5(a and b) shows the antibacterial activity of hybrid nanomaterials. The bactericidal activity of Fe<sub>2</sub>O<sub>3</sub> PANI-Cyst (0.02 and 0.05) at 10 µg/mL, with the following results: the value of inhibition zone is listed in Table 2.

**Table 2: The value of inhibition zone (gram-negative and positive).**

Doping	Type of bacteria	1000%	750%	500%	250%
Fe <sub>2</sub> O <sub>3</sub> 0.05mg	E-coli (gram negative)	24mm	26mm	12mm	10mm
	S. aureus (gram positive)	25mm	20mm	4mm	2mm
	Candida	20mm	14mm	10mm	4mm
Fe <sub>2</sub> O <sub>3</sub> 0.02mg	E-coli (gram negative)	20mm	14mm	12mm	10mm
	S. aureus (gram positive)	30mm	10mm	Zero	Zero

Compared to a previous study the effect of one of the aniline compounds (PANI) (with concentrations of 250 and 500 µg/mL) on (with concentrations of 250 and 500 µg/mL) on the same types of bacteria displayed moderate activity against both bacterial strains that the inhibition zone diameter reached (12 mm) on E. coli and (10 mm) on candida while no inhibition S. aureus [16, 17].

Due to a multitude of variables, including electrostatic adsorption between Fe<sub>2</sub>O<sub>3</sub>/PANI nanocomposites molecules and bacterium cells [17], the Fe<sub>2</sub>O<sub>3</sub>/PANI composite exhibits antibacterial action against all species of bacteria. As a result of the composite's impact and the presence of silver nanoparticles, it is known as the best antibacterial agent. Nanoparticles interact with bacteria's cell walls and cytoplasmic membranes, causing the bacteria's cell wall to burst and the bacteria to die. In general, the spherical morphology of Fe<sub>2</sub>O<sub>3</sub>/PANI nano composites may be critical for the antibacterial activity of the composite.

**Figure 5(a): The statistics of the inhibition zone.**

Clearly, the spherical nano porous particles can enter cells via membrane pores. Other types of structured nanoparticles may have difficulty entering cells. The nano composite may interact with the surface of the cell membrane, impairing its power functions (permeability and respiration), or it may degrade within the cell, reacting with sulfur and phosphorous-containing DNA and proteins [17, 18].

The accumulation of  $\text{Fe}_2\text{O}_3$ -PANI-Cys on the bacteria's surface damaged the integrity of the cell membrane and altered its shape. The hybrid biomaterial may release ions that interact with sulfur-related membrane proteins and alter the cell membrane's permeability. Due to the direct interaction of the released ions with the membrane proteins, the released ions may improve cell membrane permeability by perforating and hole-forming bacterium membranes [19].

Molecular architecture can be used to change PANI's features., making it a good option for making antibacterial medications. PANI's electrochemical switching property aids in the transport of dopant ions through cell membranes. PANI's unique redox characteristics also allow for regulated ionic transport through the polymer membrane to the cells, resulting in improved antibacterial effects [20].

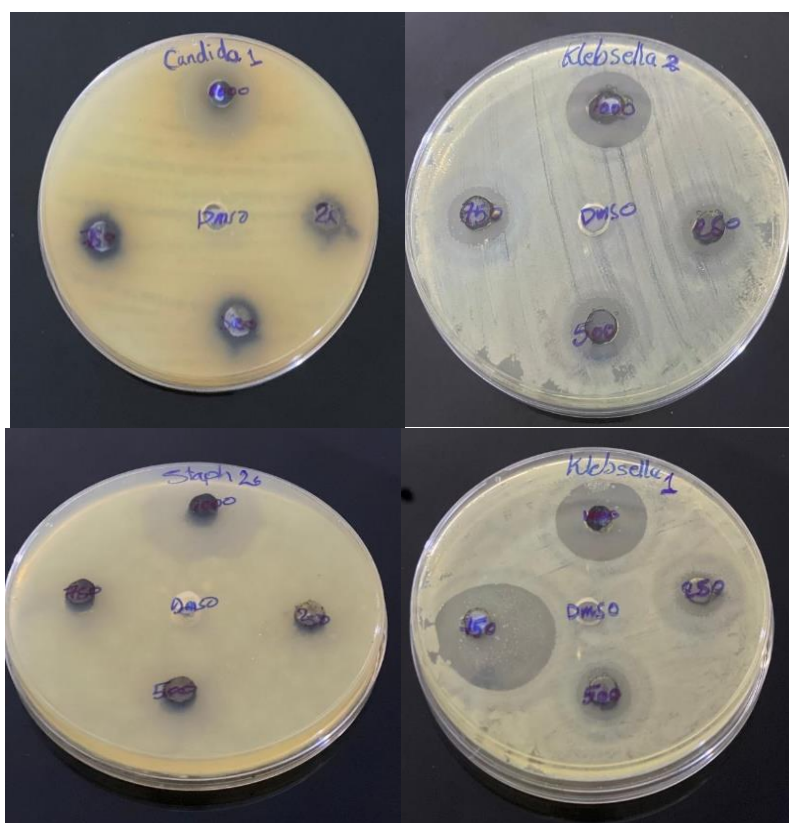


Figure 5(b): The bacterial activity (Agar Well Diffusion Method) for  $\text{Fe}_2\text{O}_3$  PANI-Cyst.

#### 4. Conclusions

Chemical polymerization is one of the simplest and most cost-effective ways to produce conductive polymers. The FTIR data revealed that the bonds are well-bonded, and the essential polymer bonds could be identified. The polymer has pores, and its granular size is (22.9- 46.09), according to FESEM analysis. Examining the conductive polymer (PANI) efficacy and its effect on reducing the inhibition zone it is concluded that the polymer can effectively kill bacteria.

## Acknowledgments

The authors acknowledge the Department of Physics, College of Science, and University of Baghdad for completing this research work.

## Conflict of interest

The authors declare that they have no conflict of interest.

## References

1. Yin C., Pan C., Liao X., Pan Y., and Yuan L., *Regulating the interlayer spacing of vanadium oxide by in situ polyaniline intercalation enables an improved aqueous zinc-ion storage performance*. ACS Applied Materials and Interfaces, 2021. **13**(33): pp. 39347-39354.
2. Shaban M., Rabia M., Fathallah W., El-Mawgoud N.A., Mahmoud A., Hussien H., and Said O., *Preparation and characterization of polyaniline and Ag/polyaniline composite nanoporous particles and their antimicrobial activities*. Journal of Polymers and the Environment, 2018. **26**(2): pp. 434-442.
3. Shuai C.-X., He Y., Su P., Huang Q., Pan D., Xu Q., Feng D., and Jiang Y., *Integration of PEGylated polyaniline nanocoatings with multiple plastic substrates generates comparable antifouling performance*. Langmuir, 2020. **36**(31): pp. 9114-9123.
4. Qi X., Lu Z., You E.-M., He Y., Zhang Q.-e., Yi H.-J., Li D., Ding S.-Y., Jiang Y., and Xiong X., *Nanocombing Effect Leads to Nanowire-Based, in-Plane, Uniaxial Thin Films*. ACS Nano, 2018. **12**(12): pp. 12701-12712.
5. Lee J., Kalin A.J., Yuan T., Al-Hashimi M., and Fang L., *Fully conjugated ladder polymers*. Chemical Science, 2017. **8**(4): pp. 2503-2521.
6. Zhou T., Liang X., Wang P., Hu Y., Qi Y., Jin Y., Du Y., Fang C., and Tian J., *A hepatocellular carcinoma targeting nanostrategy with hypoxia-ameliorating and photothermal abilities that, combined with immunotherapy, inhibits metastasis and recurrence*. ACS Nano, 2020. **14**(10): pp. 12679-12696.
7. Thangudu S., Kulkarni S.S., Vankayala R., Chiang C.-S., and Hwang K.C., *Photosensitized reactive chlorine species-mediated therapeutic destruction of drug-resistant bacteria using plasmonic core-shell Ag and AgCl nanocubes as an external nanomedicine*. Nanoscale, 2020. **12**(24): pp. 12970-12984.
8. Liu Y., Yang Z., Huang X., Yu G., Wang S., Zhou Z., Shen Z., Fan W., Liu Y., and Davisson M., *Glutathione-responsive self-assembled magnetic gold nanowreath for enhanced tumor imaging and imaging-guided photothermal therapy*. ACS Nano, 2018. **12**(8): pp. 8129-8137.
9. Barbero C., Salavagione H.J., Acevedo D.F., Grumelli D.E., Garay F., Planes G.A., Morales G.M., and Miras M.C., *Novel synthetic methods to produce functionalized conducting polymers I. Polyanilines*. Electrochimica Acta, 2004. **49**(22-23): pp. 3671-3686.
10. Dong W., Li Y., Niu D., Ma Z., Gu J., Chen Y., Zhao W., Liu X., Liu C., and Shi J., *Facile synthesis of monodisperse superparamagnetic Fe<sub>3</sub>O<sub>4</sub> Core and hybrid and Au shell nanocomposite for bimodal imaging and photothermal therapy*. Advanced materials, 2011. **23**(45): pp. 5392-5397.
11. Li L., Liu Y., Hao P., Wang Z., Fu L., Ma Z., and Zhou J., *PEDOT nanocomposites mediated dual-modal photodynamic and photothermal targeted sterilization in both NIR I and II window*. Biomaterials, 2015. **41**: pp. 132-140.

12. Kanicki J. and Skotheim T., *Handbook of conducting polymers*. Dekker, New York, 1986. **543**.
13. Jaque D., Maestro L.M., del Rosal B., Haro-Gonzalez P., Benayas A., Plaza J., Rodríguez E.M., and Solé J.G., *Nanoparticles for photothermal therapies*. Nanoscale, 2014. **6**(16): pp. 9494-9530.
14. Amano K., Ishikawa H., Kobayashi A., Satoh M., and Hasegawa E., *Thermal stability of chemically synthesized polyaniline*. Synthetic Metals, 1994. **62**(3): pp. 229-232.
15. Ibarra L., Yslas E., Molina M., Rivarola C., Romanini S., Barbero C., Rivarola V., and Bertuzzi M., *Near-infrared mediated tumor destruction by photothermal effect of PANI-Np in vivo*. Laser Physics, 2013. **23**(6): pp. 066004-066007.
16. Gao D., Gao L., Zhang C., Liu H., Jia B., Zhu Z., Wang F., and Liu Z.J.B., *A near-infrared phthalocyanine dye-labeled agent for integrin  $\alpha\beta 6$ -targeted theranostics of pancreatic cancer*. 2015. **53**: pp. 229-238.
17. Mattioli-Belmonte M., Giavaresi G., Biagini G., Virgili L., Giacomini M., Fini M., Giantomassi F., Natali D., Torricelli P., and Giardino R., *Tailoring biomaterial compatibility: in vivo tissue response versus in vitro cell behavior*. The International Journal of Artificial Organs, 2003. **26**(12): pp. 1077-1085.
18. Laurencin C.T. and Elgendy H., *The biocompatibility and toxicity of degradable polymeric materials: implications for drug delivery*. Site specific drug delivery. New York: Wiley, 1994: pp. 27-46.
19. Collazos-Castro J.E., Polo J.L., Hernández-Labrado G.R., Padiá-Cañete V., and García-Rama C., *Bioelectrochemical control of neural cell development on conducting polymers*. Biomaterials, 2010. **31**(35): pp. 9244-9255.
20. Ravichandran R., Sundarrajan S., Venugopal J.R., Mukherjee S., and Ramakrishna S., *Applications of conducting polymers and their issues in biomedical engineering*. Journal of the Royal Society Interface, 2010. **7**(suppl\_5): pp. S559-S579.

## التحضير والتوصيف للنشاط المضاد للميكروبات للجسيمات النانوية المركبة من بولي انيلين واوكسيد الحديد

نذير ابراهيم محمد<sup>1</sup>، سلمى محمد حسن<sup>1</sup>، خالد جمعة خليل<sup>2</sup>

<sup>1</sup>ا قسم الفيزياء، كلية العلوم، جامعة بغداد، بغداد، العراق

<sup>2</sup>المركز العراقي لبحوث السرطان والوراثة الطبية، الجامعة المستنصرية، بغداد، العراق

### الخلاصة

تم استخدام طريقة البلمرة المؤكسدة لإنشاء مزيج جزيئات متناهية الصغر من البوليانيلين (PANI) و  $Fe_2O_3 / PANI$ . تم استخدام طرق توصيف مختلفة للتحقيق في الهياكل الهيكلية والمورفولوجية والتركيبات النانوية  $Fe_2O_3 / PANI$ . تدعم النتائج تخليق الجسيمات النانوية متعددة البلورات PANI و  $Fe_2O_3 / PANI$  الجسيمات النانوية الكروية. يتم اختبار البكتيريا موجبة الجرام للنشاط المضاد للبكتيريا. تم استخدام كميات مختلفة من الجسيمات النانوية PANI ومركبات  $Fe_2O_3 / PANI$  النانوية لاختبار المكورات العنقودية الذهبية والبكتيريا سالبة الجرام والإشريكية القولونية وأنواع المبيضات. PANI لها خصائص مضادة للجراثيم ضد جميع الكائنات الحية الدقيقة التي تم اختبارها. من ناحية أخرى، فإن مركبات  $Fe_2O_3 / PANI$  لها نشاط مضاد للجراثيم أعلى، كما يتضح من منطقة التثبيط. مناطق التثبيط البكتيري موجودة في *S. aureus* (موجبة)، والإشريكية القولونية تعمل بشكل جيد. مع زيادة تركيزات مركبات الجسيمات النانوية  $Fe_2O_3 / PANI$ ، تكون مناطق التثبيط لجميع البكتيريا أكبر، أخيرًا، يتميز النشاط المضاد للميكروبات لمركب  $Fe_2O_3 / PANI$  الجزيئي النانوية باستخدام آلية مبسطة تعتمد على التجاذب الكهروستاتيكي. تم تصنيع جزيئات الحديد النانوية بهدف اختبارها في مجال المقاومة البكتيرية.